Available online at www.sciencedirect.com
SCIENCE DIRECT®
Hearing Research 188 (2004) 57–69
HEARING RESEARCH
www.elsevier.com/locate/heares

Cochlear delays measured with amplitude-modulated tone-burst-evoked OAEs

Shawn S. Goodman [a,1], Robert H. Withnell [a,*], Egbert De Boer [b], David J. Lilly [c], Alfred L. Nuttall [d]

[a] Department of Speech and Hearing Sciences, Indiana University, 200 South Jordan Avenue, Bloomington, IN 47405, USA
[b] Academic Medical Center, KNO Room D2-226, Meibergdreef 9, 1105 AZ Amsterdam, The Netherlands
[c] VA National Center for Rehabilitative Auditory Research, Veterans Affairs Medical Center, 3710 Southwest U.S. Veterans Hospital Road, Portland, OR 97207, USA
[d] OHRC/Otolaryngology NRC 04, Oregon Health and Science University, Portland, OR 97207, USA

Received 17 August 2003; accepted 17 November 2003

Abstract

Delay times in the mammalian cochlea, whether from measurement of basilar membrane (BM) vibration or otoacoustic emissions (OAEs) have, to date, been largely based on phase-gradient estimates from steady-state responses. Here we report cochlear delays measured directly in the time domain from OAEs evoked by amplitude-modulated tone-burst (AMTB) stimuli. Measurement using OAEs provides a non-invasive estimate of cochlear delay but is confounded by the complexity of generation of such OAEs. At low to moderate stimulus levels, and provided that the stimulus frequency range does not include a region of the cochlea where there is a large change in effective reflectance, AMTB stimuli evoke an OAE with an envelope shape that is similar to the stimulus and allow a direct calculation of cochlear group delay. Such delays are commensurate with BM estimates of delay, estimates of cochlear delay inferred from neural recordings, and previous OAE measures of delay in the guinea pig. However, a nonlinear distortion mechanism, variation in effective reflectance, and intermodulation distortion products generated by the nonlinear interaction in the cochlea of the carrier and sidebands of the AMTB stimulus, may all contribute to OAEs arising with envelope shapes that are not a scaled representation of the stimulus, confounding the estimation of cochlear group delay.

Key words: Cochlea; Otoacoustic emission; Group delay; Amplitude

1. Introduction

The measurement of travel times in the mammalian cochlea has its antecedent in measurements of basilar membrane (BM) vibration and the determination of group delay from the phase gradient (e.g., Rhode, 1971; Sellick et al., 1982). Since then, various measures of cochlear delay have been reported in the literature, including signal-front delay based on data analysis in the time domain (e.g., Neely et al., 1988; Avan et al., 1990; Whitehead et al., 1996), signal-front delay estimated from time-frequency measurements (e.g., Ren et al., 2000; Konrad-Martin and Keefe, 2003), phase-gradient estimates of group delay (e.g., Robles et al., 1986; Nuttall and Dolan, 1996; Nilsen and Russell, 2000), and group delays inferred from IFFT analysis (e.g., Kalluri and Shera, 2001; Withnell et al., 2003). Measurements of BM vibration have mostly been limited to the first cochlear turn, although measurements have been reported from the fourth turn (e.g., Cooper and Rhode, 1995). In the guinea pig, such measurements from the first turn reveal cochlear group delays to the

* Corresponding author. Tel.: +1 (812) 855 9339; Fax: +1 (812) 855 5531.
E-mail addresses: goodmans@boystown.org (S.S. Goodman), rwithnel@indiana.edu (R.H. Withnell), e.d.boer@hccnet.nl (E. De Boer), lillyd@ohsu.edu (D.J. Lilly), nuttall@ohsu.edu (A.L. Nuttall).

[1] Present address: Physical Acoustics Laboratory, Boys Town National Research Hospital, 555 North 30th Street, Omaha, NE 68131, USA.

0378-5955/03/$ – see front matter © 2003 Published by Elsevier B.V.
doi:10.1016/S0378-5955(03)00375-7

region of the 18 kHz place of approximately 400 μs. Indirect measurements of cochlear delay can be inferred from neural recordings, after an ad hoc correction for synaptic delay (e.g., Goldstein et al., 1971; Allen, 1983; Gummer and Johnstone, 1984) or from neural tuning curves making use of the reciprocal relationship between filter bandwidth and delay in a cochlea that exhibits the property of minimum phase (Shera and Guinan, 2003). In the guinea pig, based on the auditory nerve fiber threshold tuning data of Tsuji and Liberman (1997), the reciprocal relationship between filter bandwidth and group delay gives cochlear delays to the 9 and 4.5 kHz regions of 640 and 960 μs (based on a 400 μs delay to the 18 kHz region and assuming a phase change across the filter bandwidth that is independent of bandwidth – see Shera and Guinan (2003)).

Both BM and neural recordings involve invasion of the structures producing the response being measured. Additionally, these measures represent delays to a fixed point on the BM. Measurements using otoacoustic emissions (OAEs) provide a non-invasive estimate of cochlear delay but are confounded by the complexity of generation of such OAEs. OAE measures of delay represent the delay of the global cochlear response and not just that of a fixed point on the BM. For OAEs, energy propagation in the cochlea has been portrayed as consisting of a round-trip delay, i.e., a delay relative to the stimulus for that particular frequency to reach its characteristic frequency (CF) place, and the delay for the OAE arising in the cochlea in the region of CF to reach the ear canal (Neely et al., 1988).

OAEs have been described as arising from one of two mechanisms: a place-fixed mechanism and a wave-fixed mechanism (Kemp, 1986). The place-fixed mechanism is now understood in terms of the theory propounded by Zweig and Shera, the OAE arising from reflections from impedance perturbations randomly distributed along the BM, predominantly from wavelets scattered from the peak region of the traveling wave (Zweig and Shera, 1995; Shera, 2003). Such an OAE has been shown to have a cochlear delay for stimulus levels of ~40 dB sound pressure level (SPL) that is commensurate with a round-trip delay with the OAE arising from the peak region of the traveling wave (Shera and Guinan, 2003). The wave-fixed mechanism involves the OAE arising from a nonlinear wave-related interaction on the BM; such a component may not have a delay equal to the round-trip delay to the CF place. For instance, if this type of OAE arises as a result of energy added to the BM by the cochlear amplifier, then the locus of origin may be basal to the peak of the traveling wave.

Measurement of cochlear delay in the time domain using OAEs has been restricted to signal-front delays. Here we describe cochlear group delays in the guinea pig measured using amplitude-modulated tone-burst (AMTB)-evoked OAEs as a function of both stimulus level and frequency.

1.1. Amplitude modulation and group delay

For the propagation of a signal $F(t)$ through a dispersive medium such as the cochlea, the effects of such dispersion on the signal envelope can be characterized by expanding the phase ϕ of the signal envelope evaluated at the signal or carrier frequency ω_c as a Taylor series:

$$\phi(\omega) = \phi(\omega_c) + [d\phi/d\omega]_{\omega_c}(\omega-\omega_c)+ 0.5[d^2\phi/d\omega^2]_{\omega_c}(\omega-\omega_c)^2 + \ldots \quad (1)$$

The first term in the expansion is a phase offset. The second term is the group delay[2] of the signal envelope. The third term produces signal envelope broadening and reduction in the amplitude of the signal envelope with time (total energy remains constant) (Elmore and Heald, 1969).

If the signal $F(t)$ is amplitude modulated over time, i.e.,

$$A(t) = F(t)\cdot\cos(\omega_m t)$$

where $\omega_m < \omega_c$ ω_m is the modulation frequency (2)

then calculation of group delay is simplified to the phase shift in the envelope of the modulation between stimulus and OAE, the effect of cochlear dispersion on the envelope of the modulator being characterized using Eq. 1.

The technique of using an amplitude-modulated signal to calculate group delay dates back to Nyquist and Brand (1928) and the calculation of telephone-line delays. In hearing research, examples of using this technique include calculating cochlear group delay from spiral ganglion cell recordings (Gummer and Johnstone, 1984) and group delays of scalp recorded auditory-evoked potentials (Dolphin and Mountain, 1992).

In order for amplitude-modulated waves to propagate unchanged through a medium, the group velocity must be independent of frequency over the frequency range $(\omega_c-\omega_m)$ to $(\omega_c+\omega_m)$ (Elmore and Heald, 1969). This is equivalent to saying that the second-order term in Eq. 1 is small relative to the first-order term. BM measurements from the first cochlear turn of the guinea

[2] Group delay is a measure of the delay of the envelope of a signal and not of the carrier signal, the delay of the carrier signal being the phase delay (Papoulis, 1962). The group delay gives the 'displacement of … [the] center of gravity' (Papoulis, 1962, p. 135) of the signal envelope. Mathematically, the group delay (τ_g) is given by $\tau_g = d\phi/d\omega$;, i.e., the rate of change of phase with frequency at the signal frequency.

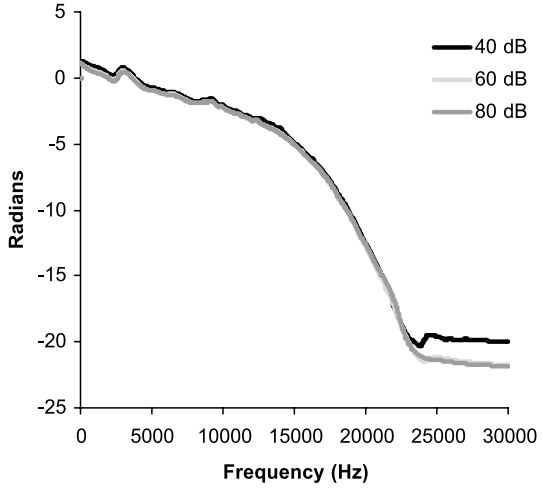

Fig. 1. BM phase versus frequency recorded from the first turn of the guinea pig cochlea in response to 40, 60 and 80 dB SPL tones.

pig (see Fig. 1) suggest it is reasonable to assume this is the case, i.e., in Fig. 1 for data from one animal group delay $d\phi/d\omega$ does not vary significantly over a frequency range that includes 750 Hz either side of the CF of approximately 18.5 kHz ($r^2 \geq 0.999$).

The group delay (τ) for an amplitude-modulated signal can be obtained from the phases of the sideband frequencies of the OAE after compensating for the stimulus (see Nyquist and Brand, 1928), i.e.,

$$\tau = [\phi_{(\omega_c+\omega_m)} - \phi_{(\omega_c-\omega_m)}]/(2\omega_m) \quad (3)$$

Alternatively, as has been done in this study, the group delay can be calculated directly in the time domain as the shift in the envelope of the modulation between the stimulus and OAE.

2. Materials and methods

2.1. Animal surgery

2.1.1. OAE measurements

Albino guinea pigs (300–650 g) were anesthetized with Nembutal (30–35 mg/kg intraperitoneally (i.p.)) and atropine (0.06–0.09 mg i.p.), followed approximately 15 min later by Hypnorm (0.1–0.15 ml intramuscularly (i.m.)). Anesthesia was maintained with supplemental doses of Nembutal and Hypnorm. In a number of animals, pancuronium (0.15 ml i.m.) was administered to reduce physiological noise associated with spontaneous muscle contractions. Guinea pigs were tracheotomized and mechanically ventilated on carbogen (5% CO_2 in O_2) with body rectal temperature maintained at approximately 37.5°C. The head was positioned using a custom-made head holder that could be rotated for access to the ear canal. Heart rate was monitored throughout each experiment. The bulla was opened dorsolaterally and a silver wire electrode placed on the round window niche for the recording and monitoring of the compound action potential (CAP). A plastic tube was placed in the bulla opening to ensure that the bulla was adequately ventilated, although no attempt was made to seal the bulla. Experimentation on animals used in this study was approved by Indiana University Bloomington Animal Care and Use Committee.

Results are reported from 36 animals, experiments having been conducted on a larger number of animals to achieve this data set. Data were taken from animals with CAP thresholds within laboratory norms.

2.1.2. BM measurements

Pigmented guinea pigs (Strain 2, NCR, obtained from the Charles River Laboratory) were used for the BM mechanical studies. The animals were housed in American Association for Accreditation of Laboratory Animal Care approved facilities and the Committee on the Use and Care of Animals at Oregon Health Sciences University approved experimental protocols.

The animals were anesthetized with ketamine (40 mg/kg, i.m.) and xylazine (10 mg/kg, i.m.). The auditory bulla was opened to expose the cochlea and the middle ear muscle tendons were transected. The guinea pig's head was firmly fixed in a head holder. A wire placed on the round window was used to monitor the CAP signal evoked by tone bursts. An N_1 level of 10 μV was used as the threshold criterion.

An opening (300 μm diameter) was made on the lateral wall of the scala tympani of the basal cochlear turn for measurements of the BM velocity. Gold-coated glass beads (20 μm diameter) were placed on the BM to serve as reflective objects for the laser beam of the laser Doppler velocimeter (Polytec OFV-1101) that was coupled to a compound microscope. The specific gravity of the gold-coated glass beads was approximately 2.8.

Results are reported from 11 animals, experiments having been conducted on a larger number of animals to achieve this data set. Data are typically taken from experiments on animals having less than 10 dB of hearing loss in the 17 kHz region.

2.2. Signal generation and data acquisition

2.2.1. OAE measurements

SFOAEs were recorded with stimulus delivery and response acquisition computer controlled using custom software and a Card Deluxe soundcard. Methods for stimulus delivery and response acquisition have been described previously (Withnell et al., 1998; Withnell

and Yates, 1998). Briefly, the acoustic stimulus was delivered by a Beyer DT48 loudspeaker placed approximately 4 cm from the entrance to the ear canal. Ear canal sound pressure recordings were made by a Sennheiser MKE 2-5 electrostatic microphone fitted with a metal probe tube (1.2 mm long, 1.3 mm inside diameter (i.d.), 1500Ω acoustic resistor) positioned approximately 2 mm into the ear canal. The microphone and probe tube combination was calibrated against a Bruel and Kjaer 1/8 inch microphone. The output from the probe tube microphone was amplified 20 dB, high-pass filtered (0.64 kHz, four poles Butterworth) and transmitted as a balanced input to one of the analog input channels of the computer soundcard (total gain 30 dB) where it was subsequently digitized in ~46 or 93 ms epochs at a rate of 44.1 or 48 kHz (2048 or 4096 points for the FFT).

The stimuli were digitally generated AMTBs of 25, 35 or 45 ms duration with 3 or 5 ms cosine ramps, the analog output buffered by a Tucker–Davis Technologies HB6 loudspeaker buffer amplifier. Stimulus frequencies were approximately 4.5, 9 and 18 kHz. Modulation rates were either 86 or 172 Hz. Stimulus levels ranged from 40 to 90 dB peak SPL (pSPL). SFOAEs were extracted using the nonlinear extraction paradigm (Kemp et al., 1990) from the ear canal sound pressure recordings made in response to a stimulus train with a 6 dB difference between the lower level (probe level) and higher level (reference level) stimuli. Subsequent to recording the ear canal SPL and extracting the SFOAE, each SFOAE was digitally filtered using a zero-phase 500-point FIR filter centered at the carrier frequency with a bandwidth of $2f_m$+500 Hz to improve the signal to noise ratio of the SFOAE (where f_m was the modulation frequency). Note that narrow-band filtering of the OAE with a non-causal filter will cause a ripple in the time-domain OAE waveform (it is not present in the raw data).

Measurements in a cavity suggested that intermodulation distortion produced by harmonics of the stimulus tone at the SFOAE frequency was more than 20 dB below the level of the measured OAE for the highest level of stimulus used in this study.

2.2.2. BM measurements

The acoustic stimulus consisted of a pseudo-random noise signal (20 ms duration) output from a circular buffer on a D/A converter board. This stimulus was used to drive a condenser microphone (B&K type 4134, 0.5″ diameter) serving as a loudspeaker that was coupled to the animal's ear. Synchronously with the D/A conversions, an A/D converter sampled the signal from the laser velocimeter. The BM response to the pseudo-random noise signal was averaged from more than 1000 repetitions. The averaged velocity signal was analyzed with custom software to derive 'transfer functions' of BM motion. See De Boer and Nuttall (1997) for analysis details.

2.3. OAE data analysis

Group delay was calculated by comparing the phases of cosine waves fit to the modulation envelopes of the stimuli and OAEs. Hilbert transforms of the stimuli and OAEs produced analytic signals, the magnitudes of which were the respective envelopes. Due to the presence of onset and offset ramps, only the middle portions of the envelopes of the stimuli and OAEs could be accurately fit with cosine waves of constant amplitude and DC offset. Therefore, in order to simplify the fitting procedure, only the middle 50% of the AMTB stimulus and OAE envelopes were used for fitting. A representative example of a waveform, its envelope, and the middle portion are shown in Fig. 2. An iterative least-squares algorithm was used to fit the envelope of the middle portion with a cosine wave. The algorithm was based on three assumptions: (i) Frequency is known and constant across the waveform being fit. In the case of an undistorted envelope, this frequency is the modulation frequency of the stimulus. (ii) The amplitude of the envelope is constant across the fitting range. (iii) DC offset is constant across the fitting range.

The group delay was calculated as

$$\tau_g = \frac{\phi_E - \phi_S}{\omega_{f_m}} \tag{4}$$

where τ_g is group delay in seconds, ω_m is the radian frequency of the cosine waves (equal to the modulation frequency of the stimulus), ϕ_S is the phase in radians of the best cosine fit to the stimulus envelope, and ϕ_E is the phase in radians of the best cosine fit to the OAE envelope.

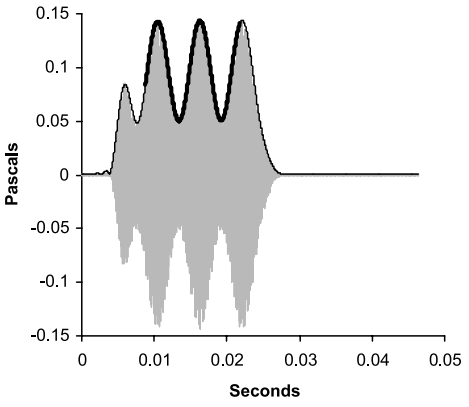

Fig. 2. A representative example of a stimulus waveform and its envelope calculated via the Hilbert transform. An iterative least-squares algorithm was used to fit the middle portion of the envelope with a cosine wave (thick black line).

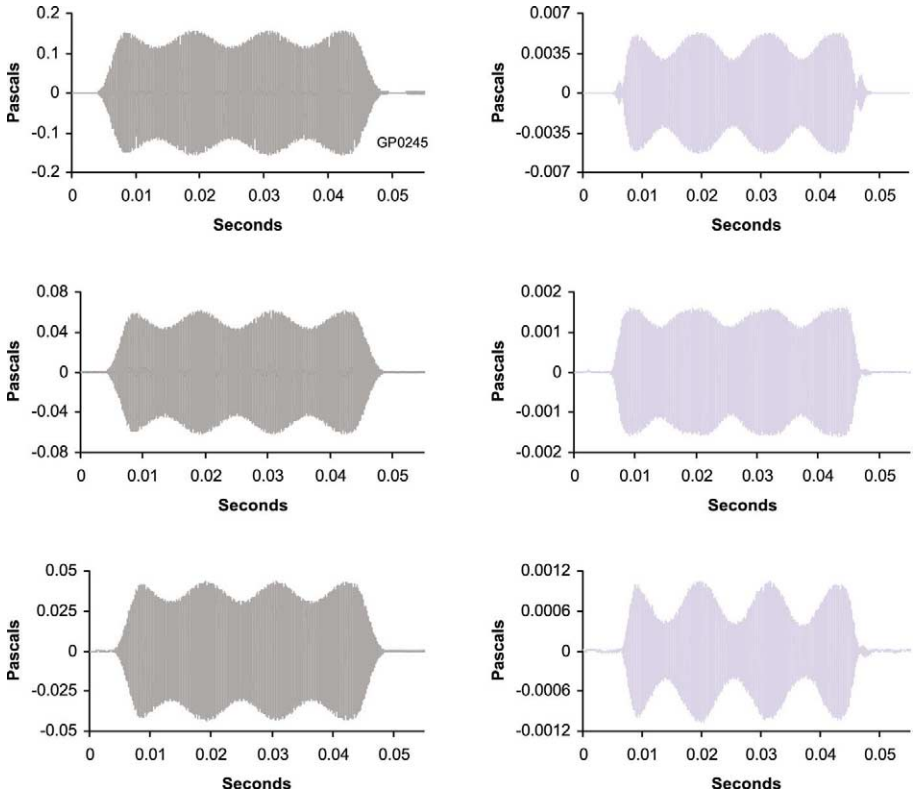

Fig. 3. Three examples of 9 kHz, 45 ms tone-burst stimuli modulated at a rate of 86 Hz stimuli (left column) and the OAEs evoked (right column). In each case, the waveform envelope shape of the OAE is similar to the stimulus with the exception that the modulation depth is different between stimulus and OAE and between OAEs. All responses were obtained from one animal but with stimulus level varied (77, 69 and 66 dB pSPL).

3. Results

3.1. AMTB-evoked OAE waveform envelope shape

The use of amplitude modulation to calculate cochlear group delay assumes that the phase is linear over the frequency range of modulation. For the modulation rates of 86 and 172 Hz used in this study, this assumption is presumably valid for the three stimulus frequencies used[3]. Fig. 3 shows three examples of OAEs obtained to 9 kHz, 45 ms tone-burst stimuli modulated at a rate of 86 Hz. In each case, the waveform envelope shape of the OAE is similar to the stimulus with the exception that the modulation depth is different between stimulus and OAE and between OAEs. Stimulus frequency is the same in each case and all responses were obtained from the same animal but with stimulus level varied (77, 69 and 66 dB pSPL). Stimulus level-dependent changes in the modulation depth of the OAE presumably occurred due to changes in the amplitude relationship between the carrier signal and the sidebands (see Section 3.2 for further discussion).

Fig. 4 shows examples of OAEs obtained from three animals in response to a 9 or 18 kHz stimulus at a modulation rate of 86 Hz and stimulus levels in the range 61–72 dB pSPL. Unlike in Fig. 3, OAE waveform envelope shape in each case is not similar to the stimulus; an increase in the number of peaks in the OAE waveform is evident in the upper and middle panels, consistent with over-modulation, while in the lower panel modulation depth is less than that of the stimulus. OAEs with 'distorted' waveform envelope shapes were a common finding.

3.2. Variation in amplitude and/or phase of the sidebands of an AMTB

The waveform envelope shape of an AMTB signal (such as an OAE) will vary if the amplitude ratio[4] is altered and/or the phase shift of the OAE relative to the stimulus is not linear over the range $f_c \pm f_m$ (Nyquist

[3] If one treats the cochlea as scale invariant, i.e., the relative bandwidth of tuning (Q) does not vary; then the phase response measured at 18 kHz on the BM can be used to infer dispersive effects at 9 and 4.5 kHz. A linear phase response over a 1500 Hz range about a CF of 18 kHz in a scale-invariant cochlea is commensurate with a linear phase response over a 750 Hz range at 9 kHz and 375 Hz at 4.5 kHz.

[4] Amplitude symmetry of sidebands and/or amplitude ratio of carrier to sidebands.

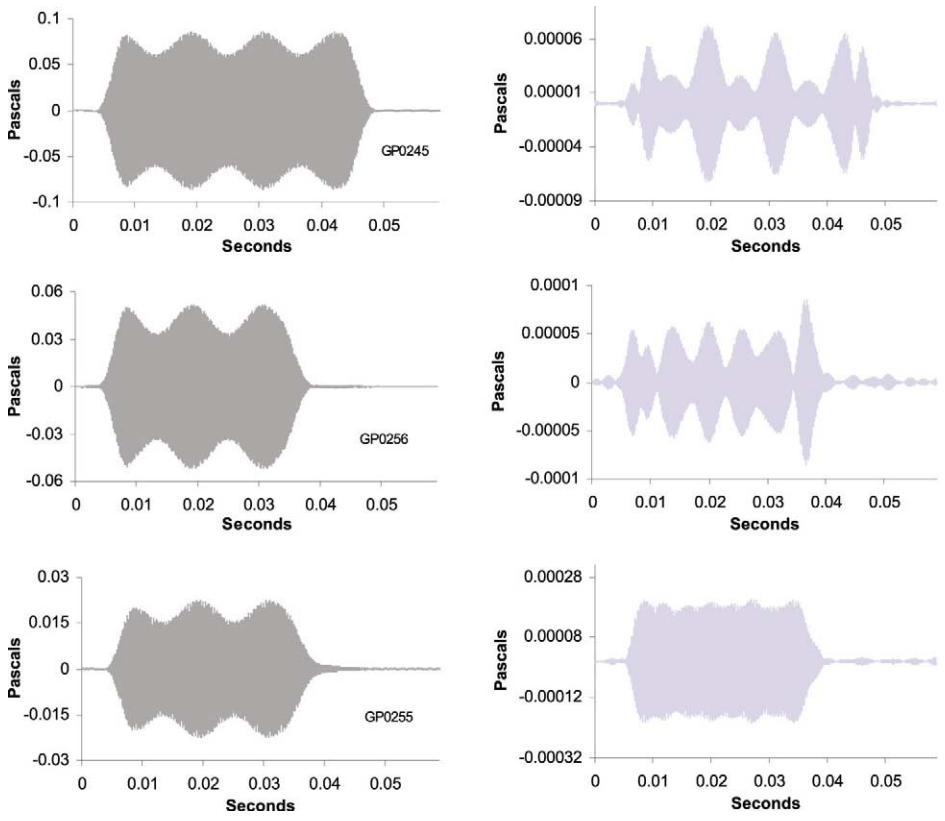

Fig. 4. Three examples of OAEs (right column) obtained in response to a 9 or 18 kHz stimulus (left column) from three different animals, the stimuli modulated at a rate of 86 Hz with stimulus levels in the range 61–72 dB pSPL. Unlike in Fig. 3, OAE waveform envelope shape in each case is not similar to the stimulus; an increase in the number of peaks in the OAE waveform is evident in the upper and middle panels, consistent with over-modulation, while in the lower panel modulation depth is less than that of the stimulus.

and Brand, 1928). This is illustrated in Fig. 5 with a simulation that shows (i) an AMTB signal with a modulation depth of 0.2 and sidebands of equal amplitude that are 14 dB less than the carrier signal but have the same phase as the carrier signal (± 0.014 radian), (ii) as per (i) but with sidebands of unequal amplitude (-4 and -14 dB re carrier signal), (iii) as per (i) but with sidebands of unequal phase (-2 and $+4$ radians re carrier signal), (iv) as per (i) but with sidebands of unequal amplitude (-4 and -14 dB) and unequal phase (-3 and 0 radians).

A difference in sideband amplitude varies the modulation depth of an AMTB without altering the position of the peaks and troughs. A phase shift that is not linear will vary the position of the peaks and troughs and the modulation depth. The degree of departure from phase linearity is given by the phase shift of the sidebands relative to the phase shift of the carrier (Nyquist and Brand, 1928), i.e.,

$$\Delta\phi = \left|\frac{\Delta\phi_{LB} + \Delta\phi_{HB}}{2} - \Delta\phi_C\right| \quad (5)$$

where $\Delta\phi$ is the deviation from linearity in radians, $\Delta\phi_{LB}$ is the phase shift of the low-frequency sideband of the OAE relative to the stimulus, $\Delta\phi_{HB}$ is the phase shift of the high-frequency sideband, and $\Delta\phi_C$ is the phase shift of the carrier.

3.3. Causes of OAE distortion

3.3.1. Two sources

SFOAEs[5] from the guinea pig have previously been shown to be a stimulus level-dependent mix of nonlinear distortion and linear reflection components (Goodman et al., 2003). The complex addition of these two components may impact on the waveform envelope shape of the OAE obtained from an AMTB stimulus if the resultant OAE sidebands vary in amplitude ratio and/or have a phase shift that is not linear ($\Delta\phi > 0$). If the reflection component dominates the composition of the OAE, then the OAE obtained would be expected to be a scaled version of the stimulus. If the nonlinear distortion component is dominant, the OAE would also be expected to be a scaled version of the stimulus, but with a delay that is not representative of an actual cochlear delay due to the wave-fixed nature of this component (in the case of a wave-fixed nonlinear compo-

[5] In response to tone-burst stimuli with no amplitude modulation.

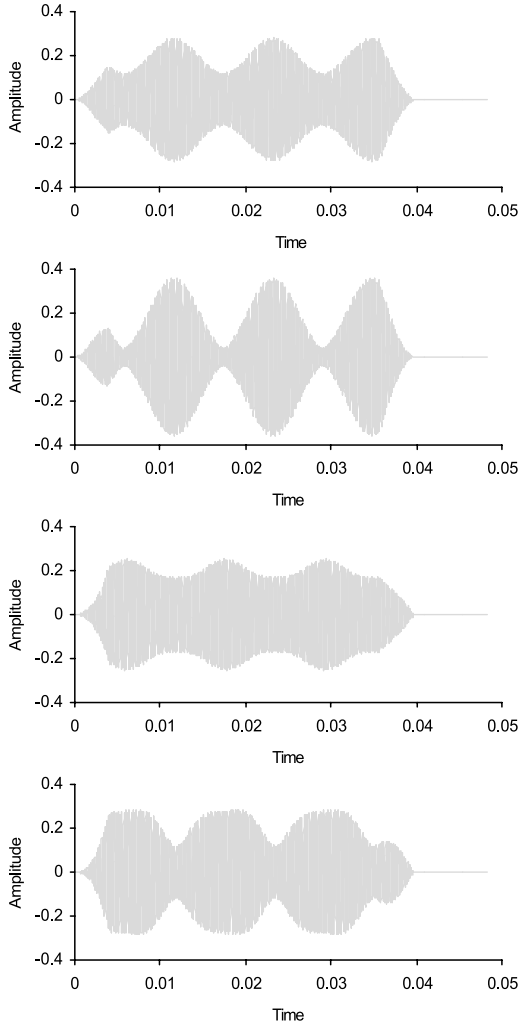

Fig. 5. Schematic of (first panel) an AMTB signal with a modulation depth of 0.2 and sidebands of equal amplitude 14 dB less than the carrier signal with the same phase as the carrier signal (±0.014 radian) (2048 point FFT, 'sampling rate' of 44 100 Hz), second panel: as per first panel but with sidebands of unequal amplitude (−4 and −14 dB re carrier signal), third panel: as per first panel but with sidebands of unequal phase (−2 and +4 radians re carrier signal), fourth panel: as per first panel but with sidebands of unequal amplitude (−4 and −14 dB) and unequal phase (−3 and 0 radians).

nent, the carrier and sidebands undergo approximately the same phase shift relative to the stimulus).

3.3.2. Variation in effective reflectance

The amplitude of the OAE nonlinear component is presumed to be approximately constant versus frequency (Talmadge et al., 2000), whereas the amplitude of the reflection component has been found to vary with frequency (Shera and Guinan, 1999; Goodman et al., 2003). This variation in SFOAE reflection component amplitude versus frequency with an associated variation in phase arises in the guinea pig cochlea presumably as a result of variation in effective reflectance with position along the cochlea (Zweig and Shera, 1995; Goodman et al., 2003). Consequently, for frequencies corresponding to amplitude minima, the amplitude ratio of the sidebands will be altered relative to the stimulus, $\Delta\phi > 0$, and the phase gradient will not reflect the cochlear delay. Variation in the amplitude ratio and phase will produce a distorted OAE waveform.

Fig. 6 shows the amplitude and phase microstructures for an OAE evoked by an AMTB stimulus, the time-domain stimulus waveform, and the OAE time-domain waveforms for 8171 and 8516 Hz, corresponding to amplitude minima and maxima respectively. For an AMTB OAE arising from the peak region of the SFOAE amplitude microstructure, the OAE waveform is a scaled representation of the stimulus but with a change in modulation index. For the OAE corresponding to an amplitude minimum, the OAE waveform is distorted relative to the stimulus (it has twice as many peaks as the stimulus). Such waveform distortion could arise due to changes in the amplitudes and phases of the sidebands associated with a variation in effective reflectance over the frequency range encompassed by the sidebands.

3.3.3. Intermodulation distortion

The nonlinear interaction on the BM of the stimulus tones that make up the AMTB produces intermodulation distortion products. These include distortion products at the higher-frequency sideband and lower-fre-

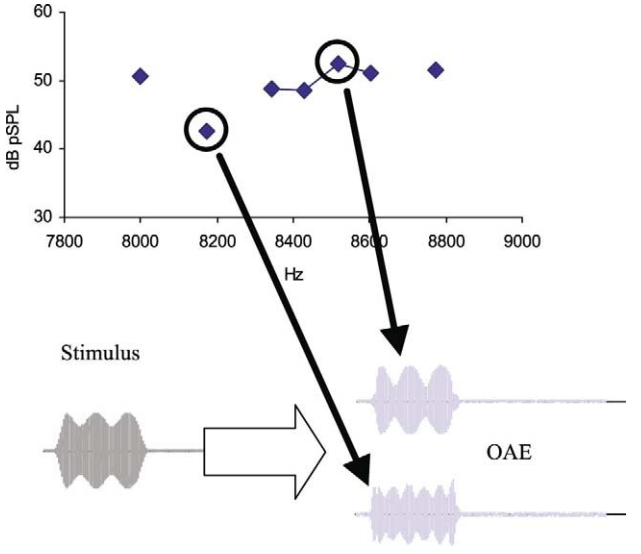

Fig. 6. Amplitude and phase microstructure for an OAE evoked by an AMTB stimulus, the time-domain stimulus waveform, and the OAE time-domain waveforms for the OAEs at 8171 and 8516 Hz, corresponding to amplitude minima and maxima respectively. For an AMTB OAE arising from the peak region of the SFOAE amplitude microstructure, the OAE waveform is a scaled representation of the stimulus (but with a change in modulation index). For the OAE corresponding to an amplitude minimum, the OAE waveform is distorted relative to the stimulus.

quency sideband arising from the nonlinear interaction of the carrier with the opposing sideband. Such nonlinear distortion products, if of sufficient amplitude, would vary the amplitude and phase of the sidebands contributing to the AMTB SFOAE, producing distortion of OAE waveform envelope shape.

3.4. AMTB-evoked OAE group delay

Distorted OAE waveforms contaminate estimation of group delay from the least-squares fit to a sinusoid (see Section 2.3). The origin of this distortion is further examined in Section 3.5, such distortion being present when the second-order term in Eq. 1 for the phase of the envelope of the AMTB OAE becomes significant relative to the first-order term. Group delay was calculated from that subset of data where the OAE envelope retained the sinusoidal shape of the AMTB stimulus waveform envelope, i.e., those OAEs with the same number of peaks and dips as the stimuli that evoked them. Fig. 7 shows the group delays for OAEs evoked by 4.5, 9 and 18 kHz AMTB stimuli versus stimulus

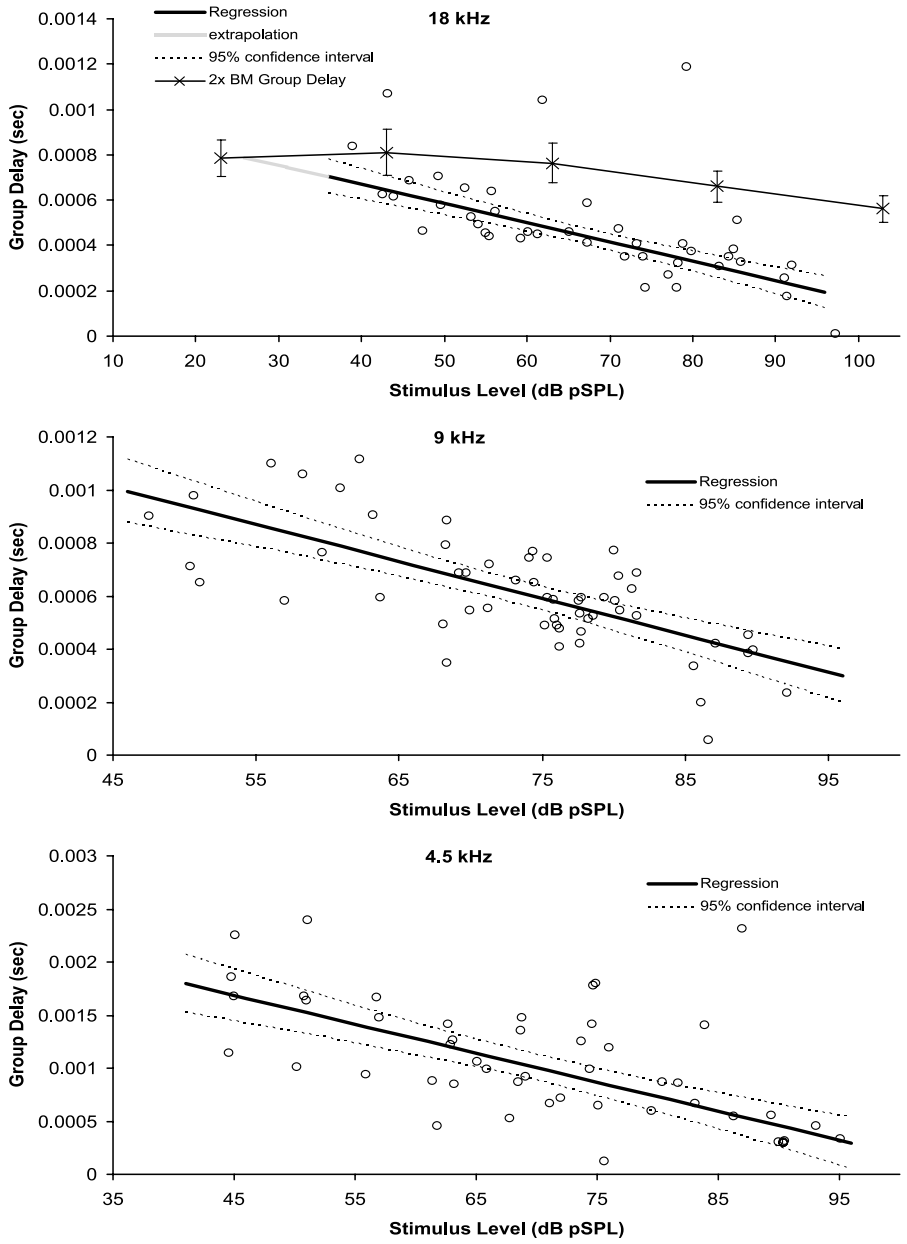

Fig. 7. Group delays for OAEs evoked by 4.5, 9 and 18 kHz AMTB stimuli versus stimulus level and the corresponding linear regression line for each set of data. Also shown on the upper panel is twice the BM group delay versus stimulus level calculated from BM laser velocimetry measurements made near the 18 kHz place. OAE regression line equations: 4.5 kHz: $y = -0.000027 \cdot x + 0.002914$, 9 kHz: $y = -0.000014 \cdot x + 0.001637$, 18 kHz: $y = -0.0000085 \cdot x + 0.001008$.

level and the corresponding bi-squares regression line for each set of data. In each case, group delay decreases with increasing stimulus level. Fig. 7, upper panel shows that group delay decreases from ~670 μs at 40 dB pSPL to 240 μs at 90 dB pSPL for an 18 kHz stimulus (based on the bi-squares regression line). Also shown on this panel is twice the BM group delay versus stimulus level calculated from BM laser velocimetry measurements made near the 18 kHz place. BM measurements represent a fixed point-source measurement. OAEs, in contrast, represent the delay of the global cochlear response and not just that of a fixed point on the BM. Extension of the regression line for the SFOAE data suggests that at some stimulus level (~25 dB pSPL) below that encompassed by the data the group delay would be approximately twice the BM delay. At low stimulus levels, SFOAEs in guinea pig have been shown to arise predominantly from a place-fixed reflection mechanism (Goodman et al., 2003) and so are a reasonable estimate of cochlear delay (this subset of data presumably excludes SFOAEs arising from regions where amplitude minima occur associated with variations in effective reflectance). At higher stimulus levels, SFOAE group delays diverge from BM group delays, BM group delays being relatively stimulus intensity invariant. At the highest stimulus levels, SFOAE group delay is expected to be confounded by OAE arising from a nonlinear distortion mechanism; SFOAEs in guinea pigs at high stimulus levels can be dominated by a nonlinear distortion mechanism (Goodman et al., 2003). The data presumably do not show delineation of delays for OAEs arising from the two mechanisms due to (i) the mixing of the two components, (ii) the data set being obtained from nine guinea pigs. Further research is necessary on individual animals to explore if such a break-point in group delay exists. The divergence of group delay between BM data and OAE data is also to be expected based on the fact that the OAE represents a global measure of cochlear delay and so delays should decrease due to a basalward shift in the excitation pattern on the BM.

Fig. 7, middle panel shows group delays in response to a 9 kHz stimulus versus stimulus level, delay values ranging from ~940 μs at 50 dB pSPL to ~380 μs at 90 dB pSPL. Fig. 7, lower panel shows group delays in response to a 4.5 kHz stimulus versus stimulus level, delay values ranging from ~1700 μs at 45 dB pSPL to ~480 μs at 90 dB pSPL. Extension of the SFOAE regression lines to 25 dB pSPL suggests a delay of 1290 μs for 9 kHz and 2240 μs for 4.5 kHz, suggestive of a group delay for the OAE in each case that is approximately twice the BM delay (based on cochlear delays of 640 μs at 9 kHz and 960 μs at 4.5 kHz (see Section 1)).

A two-octave separation between 4.5 and 18 kHz produces an SFOAE delay difference of 1700 to 630 μs for a 45 dB pSPL stimulus. With increasing stimulus level it is expected that a basalward shift in the excitation pattern on the BM should result in a decrease in delay. Based on a half-octave shift in the peak of the excitation pattern at a high stimulus level, and assuming local scaling symmetry[6], group delays of approximately 1580 and 560 μs for 4 and 18 kHz respectively would be expected[7]. At 90 dB pSPL group delay values of 450 to 300 μs were obtained. This significant disparity presumably results from the OAE arising predominantly from a nonlinear distortion mechanism at high stimulus levels (see Section 3.3.1).

Using a variant of the suppressor paradigm (Brass and Kemp, 1991, 1993), Shera and Guinan (2003) found average phase-gradient estimate of group delays for SFOAEs in response to 40 dB SPL tone bursts of approximately 710 μs at 18 kHz, 1040 μs at 9 kHz, and 1640 μs at 4 kHz[8]. Comparable data from Fig. 7, which is a time-domain measure of group delay but would be equivalent to a phase-gradient value in a linear system, gives delays of 640, 1035, and 1750 μs.

3.5. Waveform envelope shape

A 'good' envelope shape was defined as an OAE envelope that retained the sinusoidal shape of the AMTB stimulus, i.e., those OAEs with the same number of peaks and dips as the stimuli that evoked them (does not exclude those OAE waveforms with changes in modulation index). Examination of OAE waveform envelope shape in terms of the effect of a phase shift that is not linear (see Fig. 8) revealed that:

1. for $\Delta\phi > 1$ and $f_c = 18$ kHz, 70% of OAEs had distorted envelope shape while 15% had good envelope shape;
2. for $\Delta\phi > 0.7$ and $f_c = 9$ kHz, 52% of OAEs had distorted envelope shape while 5% had good envelope shape; and
3. for $\Delta\phi > 0.7$ and $f_c = 4.5$ kHz, 55% of OAEs had distorted envelope shape while 26% had good envelope shape.

It is apparent that a phase shift that is not linear is not the sole source of AMTB OAE envelope distortion and that, indeed, some OAEs retained a sinusoidal envelope shape with phase shifts that typically produced

[6] While local scaling symmetry only applies at a fixed level for the BM excitation pattern, it is suggested that the group delay scales with stimulus level because it can be thought of as the delay to the peak (~equivalent to the center of gravity) of the wave.

[7] Delay = $2^{-0.5}$ times delay estimate at 25 dB pSPL.

[8] Obtained from table 1 of Shera and Guinan (2003), i.e., group delay = $3.56 \cdot f^{0.44}/1000 \cdot f$, where f is expressed in kHz ($\tau = N_{sfoae}/f_{CF}$).

distorted waveforms. However, the inclusion of variation in the amplitude ratio as a parameter that could impact on OAE envelope shape (see Section 3.2) did not improve the identification of good versus distorted waveform envelope shapes. Also, apparent from Fig. 8, stimulus level does not appear to affect OAE envelope shape, as one might expect if intermodulation distortion (Section 3.3.3) contributed to a variation in amplitude and/or phase of the OAE sidebands.

Distorted OAE waveform envelopes compromise the calculation of group delay. As illustrated in Fig. 5, a phase shift that is not linear produces a shift in the position of the peaks and troughs, invalidating the use of a shift in the waveform envelope as a measure of group delay. It is evident, though, that not all examples of distortion of the OAE waveform envelope are explained by a phase shift that is not linear.

4. Discussion

Significant advances in our understanding of the mechanics of mammalian cochlear function have been made in the past 30 years or so, precipitated by the application of the Mossbauer technique to the measurement of BM vibration in 1967 (Johnstone and Boyle, 1967). William Rhode subsequently showed that BM vibration growth is compressively nonlinear (Rhode, 1971), such nonlinearity manifesting psycho-acoustically as the perception of intermodulation distortion products (Tartini's tones) and physiologically as sound radiating from the ear, or OAEs (Kemp, 1978). Thomas Gold, in 1948, predicted that a cellular motor must exist in the cochlea to provide for the sensitivity and frequency selectivity observed in humans (Gold, 1948), Duck On Kim and colleagues subsequently demonstrating that a cochlear model with a power source or active mechanical behavior reasonably accurately predicted the BM measurements of Rhode (Kim et al., 1980; Neely and Kim, 1983, 1986). Nonlinear behavior has since been combined with active properties in various cochlear models to form the basis of our current understanding of cochlear mechanical function (e.g., Zwicker, 1986; Chadwick, 1998; de Boer and Nuttall, 2000; Lim

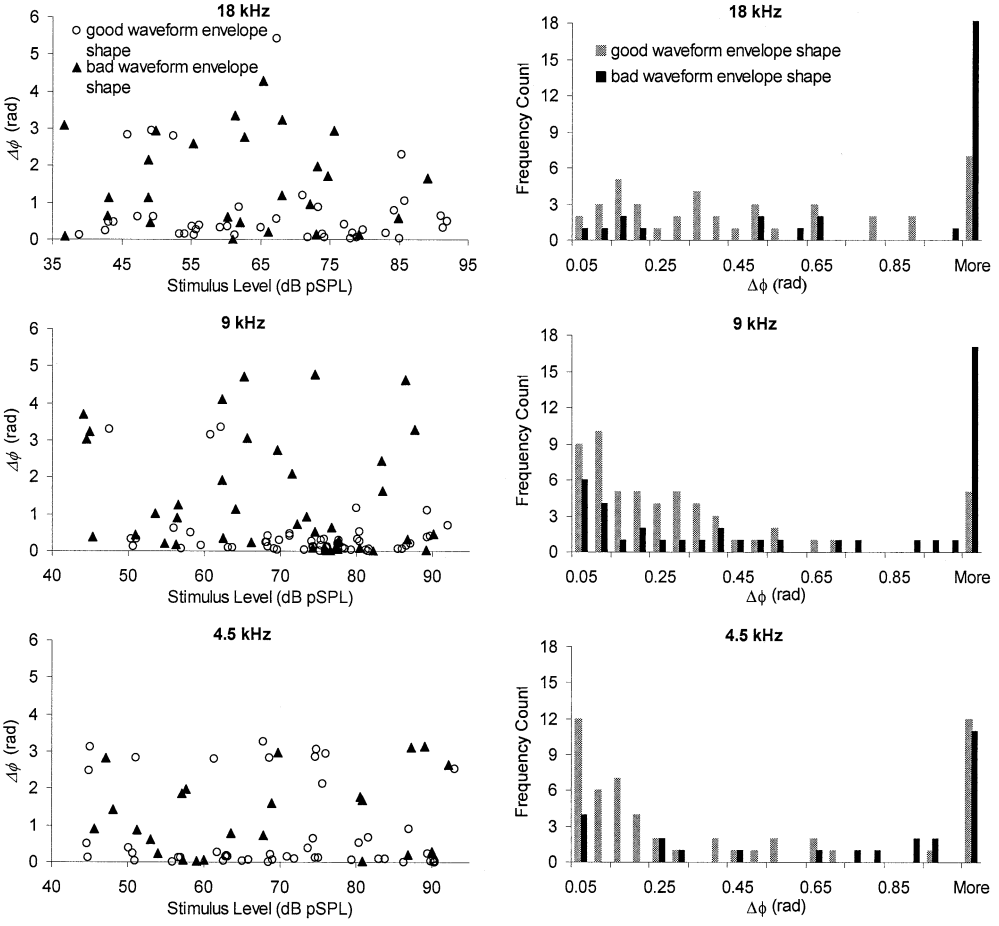

Fig. 8. Phase shift as a function of stimulus level at each of the three stimulus frequencies for each of the OAEs obtained. Good versus bad OAE envelope shape (see text) is identified.

and Steele, 2002). However, much remains to be understood about the mechanics of the cochlea, including the manner and form of energy propagation in the cochlea, the location of the putative cellular motor and how it works (for a review, see Withnell et al., 2002), and the source of cochlear inhomogeneity. OAEs, either directly or indirectly, are associated with cochlear mechanical amplification, and provide a non-invasive window into cochlear mechanics. No study has yet reported OAEs measured simultaneously with BM motion but the link between OAEs and cochlear mechanics has been established: Powers et al. (1995) showed that subsequent to producing a punctate lesion in the cochlea, a spontaneous OAE was measured concomitant with an increase in neural firing. The parsimonious explanation for this is that the increased neural firing rate was due to an increase in BM vibration associated with the presence of the spontaneous OAE. Complicating the use of OAEs as a tool to investigate cochlear mechanics is the fact that they have a complex origin (DPOAEs: Brown et al., 1996; Heitmann et al., 1998; Talmadge et al., 1999; Kalluri and Shera, 2001; Withnell et al., 2003; SFOAEs: Goodman et al., 2003; Talmadge et al., 2000; TEOAEs: Yates and Withnell, 1999; Withnell et al., 2000).

Delay times in the cochlea, whether it be from BM or OAE measurements have, to date, been largely based on phase-gradient estimates from steady-state responses and not directly measured time delays (Tubis et al., 2000). Here we report cochlear delays measured directly in the time domain from OAEs evoked by AMTB stimuli. At low to moderate stimulus levels, and provided that the stimulus frequency range does not include a region of the cochlea where there is a large change in effective reflectance, AMTB stimuli appear to evoke an OAE with an envelope shape that is similar to the stimulus and allows a direct calculation of cochlear group delay. Such delays are commensurate with BM estimates of delay, estimates of cochlear delay inferred from neural recordings, and previous OAE measures of delay in the guinea pig (Shera and Guinan, 2003).

Comparison of OAE delay with BM data can only be meaningful when the OAE arises from what approximates a point source and so is analogous to BM measurements (unless one has a good model that related the two). The data of Fig. 7 do not suggest OAE delays asymptoting to a constant value at low stimulus levels as would be expected when the OAE arises from, effectively, a point-source location. Measurement of OAEs using the nonlinear extraction paradigm appears to preclude measuring SFOAEs below about 40 dB pSPL due to signal-to-noise considerations. However, extension of the regression lines fitted to the data in Fig. 7 suggests that at low stimulus levels ($\sim$25 dB pSPL) the group delay for OAEs measured at 4.5, 9 and 18 kHz approximates a round-trip delay based on BM data (measured at approximately the 18 kHz CF place) or inferred from neural data at 9 and 4.5 kHz. AMTB OAE group delays measured at high stimulus levels are not representative of cochlear delay times, being confounded presumably by the OAE arising predominantly from a nonlinear distortion mechanism. The sideband and carrier frequencies for an OAE arising from a nonlinear distortion mechanism do not have phases consistent with their cochlear spatial separation; arising from a wave-fixed mechanism, phase does not accumulate with frequency for the respective components that make up the AMTB OAE.

4.1. *Place-fixed reflection OAE group delays at high stimulus levels*

At high stimulus levels the SFOAE is dominated by a nonlinear distortion mechanism (Goodman et al., 2003). OAEs arising from a place-fixed reflection mechanism provide an estimate of cochlear delay due to the phase accumulation that occurs over the range of the sideband frequencies, subject to the caveat that amplitude ratio or phase changes of the carrier and sidebands associated with intermodulation distortion products and variation in effective reflectance will confound such delay estimates. It may be possible to examine cochlear delays at high stimulus levels using AMTB OAEs, where only the reflection component is considered in the calculation. Fourier analysis and time-domain windowing of an AMTB SFOAE data set measured in small step sizes over a wide frequency range provides for separation of the nonlinear and reflection components (see Kalluri and Shera, 2001; Withnell et al., 2003; Goodman et al., 2003), allowing group delay to be determined for the reflection component. However, Goodman et al. (2003) found no level-dependent systematic change in group delay for this component (from one animal) over the stimulus range 62–86 dB pSPL.

4.2. *A 6 dB stimulus level ratio*

The nonlinear extraction paradigm (Kemp et al., 1990) used in this study to extract the OAE from the ear canal sound pressure recording isolates the OAE from the stimulus by virtue of its nonlinear growth with stimulus level. To maximize the magnitude of the OAE, it should be extracted from ear canal sound pressure recordings referenced to a high stimulus level where it has presumably saturated (Martin et al., 1988). In this study, the stimulus level ratio was only 6 dB, a value chosen not to maximize the magnitude of the OAE but to obtain a representative value of cochlear delay. With increasing stimulus level there is a basal-

ward shift in the BM excitation pattern – for OAEs evoked by greatly different stimulus levels there would be a temporal disparity in the onset of the respective OAEs.

4.3. Nonlinear extraction versus a suppression paradigm

The nonlinear extraction paradigm is dependent on saturation of the growth of the OAE for extraction of the whole OAE. If OAE growth has not saturated, as occurs at lower stimulus levels, the extracted OAE underestimates the actual OAE. The suppression paradigm of Brass and Kemp (1991, 1993) may provide for a larger OAE at low stimulus levels but has the confounding effect that an additional (suppressor) tone is added.

4.4. Conclusion

Measurement of cochlear delay times using OAEs are confounded to some extent by the complexity of their origin. OAEs arising from a nonlinear distortion mechanism, variation in effective reflectance of the OAE arising from a linear, place-fixed reflection mechanism, and intermodulation distortion products generated by the nonlinear interaction in the cochlea of the carrier and sidebands of the AMTB stimulus, may all contribute to OAEs arising with envelope shapes that are not a scaled representation of the stimulus, confounding estimation of cochlear group delay. The group delay calculated from AMTB OAEs would appear to correspond to physical cochlear delay times only when the shape of the OAE envelope is similar to the stimulus and the stimulus level is low.

Acknowledgements

This work was supported by NIH-NIDCD DC04921 (R.H.W.), NIH-NIDCD T32 DC00012 Training Grant (S.S.G.), NIHDCD DC00141 (A.L.N.), V.A. Project # C26559C (D.J.L.). Portions of this paper were presented at the Association for Research in Otolaryngology Mid-Winter Meeting, 2003. We thank Dr. Christopher Shera and two anonymous reviewers for providing valuable feedback on the manuscript and Rachel Roberts for willingly proof-reading each version and identifying the grammatical faux pas.

References

Allen, J.B., 1983. Magnitude and phase-frequency response to single tones in the auditory nerve. J. Acoust. Soc. Am. 73, 2071–2092.

Avan, P., Loth, D., Menguy, C., Teyssou, M., 1990. Evoked otoacoustic emissions in guinea pig: basic characteristics. Hear. Res. 44, 151–160.

Brass, D., Kemp, D.T., 1991. Time-domain observation of otoacoustic emissions during constant tone stimulation. J. Acoust. Soc. Am. 90, 2415–2427.

Brass, D., Kemp, D.T., 1993. Suppression of stimulus frequency otoacoustic emissions. J. Acoust. Soc. Am. 93, 920–939.

Brown, A.M., Harris, F.P., Beveridge, H.A., 1996. Two sources of acoustic distortion products from the human cochlea. J. Acoust. Soc. Am. 100, 3260–3267.

Chadwick, R.S., 1998. Compression, gain, and nonlinear distortion in an active cochlear model with subpartitions. Proc. Natl. Acad. Sci. USA 95, 14594–14599.

Cooper, N.P., Rhode, W.S., 1995. Nonlinear mechanics at the apex of the guinea-pig cochlea. Hear. Res. 82, 225–243.

De Boer, E., Nuttall, A.L., 1997. The mechanical waveform of the basilar membrane. I. Frequency modulations ('glides') in impulse responses and cross-correlation functions. J. Acoust. Soc. Am. 101, 3583–3592.

de Boer, E., Nuttall, A.L., 2000. The mechanical waveform of the basilar membrane. III. Intensity effects. J. Acoust. Soc. Am. 107, 1497–1507.

Dolphin, W.F., Mountain, D.C., 1992. The envelope following response: scalp potentials elicited in the Mongolian gerbil using sinusoidally AM acoustic signals. Hear. Res. 58, 70–78.

Elmore, W.C., Heald, M.A., 1969. Physics of Waves. Dover Publications, New York.

Gold, T., 1948. Hearing II. The physical basis of the action of the cochlea. Proc. R. Soc. Lond. Biol. 135, 492–498.

Goldstein, J.L., Baer, T., Kiang, N.Y.S., 1971. A theoretical treatment of latency, group delay, and tuning characteristics of auditory-nerve responses to clicks and tones. In: Sachs, M.B. (Ed.), Physiology of the Auditory System. National Educational Consultants, Baltimore, MD, pp. 133–141.

Goodman, S.S., Withnell, R.H., Shera, C.A., 2003. The origin of SFOAE microstructure in the guinea pig. Hear. Res. 183, 7–17.

Gummer, A.W., Johnstone, B.M., 1984. Group delay measurement from the spiral ganglion cells in the basal turn of the guinea pig cochlea. J. Acoust. Soc. Am. 76, 1388–1400.

Heitmann, J., Waldmann, B., Schnitzler, H., Plinkert, P.K., Zenner, H., 1998. Suppression of distortion product otoacoustic emissions (DPOAE) near $2f_1-f_2$ removes DP-gram fine structure – evidence for a secondary generator. J. Acoust. Soc. Am. 103, 1527–1531.

Johnstone, B.M., Boyle, A.J., 1967. Basilar membrane vibration examined with the Mossbauer Technique. Science 158, 389–390.

Kalluri, R., Shera, C.A., 2001. Distortion-product source unmixing: A test of the two-mechanism model for DPOAE generation. J. Acoust. Soc. Am. 109, 622–637.

Kemp, D.T., 1978. Stimulated acoustic emissions from within the human auditory system. J. Acoust. Soc. Am. 64, 1386–1391.

Kemp, D.T., 1986. Otoacoustic emissions, travelling waves and cochlear mechanisms. Hear. Res. 22, 95–104.

Kemp, D.T., Ryan, S., Bray, P., 1990. A guide to the effective use of otoacoustic emissions. Ear Hear. 11, 93–105.

Kim, D.O., Neely, S.T., Molnar, C.E., Matthews, J.W., 1980. An active cochlear model with negative damping in the partition: comparison with Rhode's ante- and post-mortem observations. In: van der Brink, G., Bilsen, F.A. (Eds.), Psychophysical, Physiological and Behavioral Studies in Hearing. Delft University Press, Delft, pp. 7–14.

Konrad-Martin, D., Keefe, D.H., 2003. Time-frequency analysis of transient-evoked stimulus-frequency and distortion-product OAEs: Testing cochlear model predictions. J. Acoust. Soc. Am. 114, 2021–2043.

Lim, K.M., Steele, C.R., 2002. A three-dimensional nonlinear active

cochlear model analyzed by the WKB-numeric method. Hear. Res. 170, 190–205.
Martin, G.K., Lonsbury-Martin, B.L., Probst, R., Coats, A.C., 1988. Spontaneous otoacoustic emissions in a nonhuman primate. I. Basic features and relations to other emissions. Hear. Res. 33, 49–68.
Neely, S.T., Kim, D.O., 1983. An active cochlear model showing sharp tuning and high sensitivity. Hear. Res. 9, 123–130.
Neely, S.T., Kim, D.O., 1986. A model for active elements in cochlear biomechanics. J. Acoust. Soc. Am. 79, 1472–1480.
Neely, S.T., Norton, S.J., Gorga, M.P., Jesteadt, W., 1988. Latency of auditory brain-stem responses and otoacoustic emissions using tone-burst stimuli. J. Acoust. Soc. Am. 83, 652–656.
Nilsen, K.E., Russell, I.J., 2000. The spatial and temporal representation of a tone on the guinea pig BM. Proc. Natl. Acad. Sci. USA 97, 11751–11758.
Nuttall, A.L., Dolan, D.F., 1996. Steady-state sinusoidal velocity responses of the BM in guinea pig. J. Acoust. Soc. Am. 99, 1556–1565.
Nyquist, H., Brand, S., 1928. Measurement of Phase Distortion. Bell Syst. Tech. J., 522–549.
Papoulis, A., 1962. The Fourier Integral and its Applications. McGraw-Hill Book Company, New York.
Powers, N.L., Salvi, R.J., Wang, J., Spongr, V., Qiu, C.X., 1995. Elevation of auditory thresholds by spontaneous cochlear oscillations. Nature 375, 585–587.
Ren, T., Nuttall, A.L., Parthasarathi, A.A., 2000. Quantitative measure of multicomponents of otoacoustic emissions. J. Neurosci. Methods 96, 97–104.
Rhode, W.S., 1971. Observations of the vibration of the basilar membrane in squirrel monkeys using the Mossbauer technique. J. Acoust. Soc. Am. 49 (Suppl. 2), 1218.
Robles, L., Ruggero, M.A., Rich, N.C., 1986. Basilar membrane mechanics at the base of the chinchilla cochlea. I. Input–output functions, tuning curves, and response phases. J. Acoust. Soc. Am. 80, 1364–1374.
Sellick, P.M., Patuzzi, P., Johnstone, B.M., 1982. Measurement of basilar membrane motion in the guinea pig using the Mossbauer technique. J. Acoust. Soc. Am. 72, 131–141.
Shera, C.A., 2003. Wave interference in the generation of reflection- and distortion-source OAEs. In: Gummer, A.W. (Ed.), Biophysics of the Cochlea: From Molecule to Model. World Scientific, Singapore, pp. 439–449.
Shera, C.A., Guinan, J.J., 1999. Evoked otoacoustic emissions arise by two fundamentally different mechanisms: A taxonomy for mammalian OAEs. J. Acoust. Soc. Am. 105, 782–798.
Shera, C.A., Guinan, J.J., 2003. Stimulus-frequency-emission group delay: A test of coherent reflection filtering and a window on cochlear tuning. J. Acoust. Soc. Am. 113, 2762–2772.
Talmadge, C.L., Long, G.R., Tubis, A., Dhar, S., 1999. Experimental confirmation of the two-source interference model for the fine structure of distortion product otoacoustic emissions. J. Acoust. Soc. Am. 105, 275–292.
Talmadge, C.L., Tubis, A., Long, G.R., Tong, C., 2000. Modeling the combined effects of basilar membrane nonlinearity and roughness on stimulus frequency otoacoustic emission fine structure. J. Acoust. Soc. Am. 108, 2911–2932.
Tsuji, J., Liberman, M.C., 1997. Intracellular labeling of auditory nerve fibers in guinea pig: Central and peripheral projections. J. Comp. Neurol. 381, 188–202.
Tubis, A., Talmadge, C.L., Tong, C., Dhar, S., 2000. On the relationship between the fixed-$f1$, fixed-$f2$, and fixed ratio phase derivatives of the $2f1-f2$ distortion product otoacoustic emission. J. Acoust. Soc. Am. 108, 1772–1785.
Whitehead, M.L., Stagner, B.B., Martin, G.K., Lonsbury-Martin, B.L., 1996. Visualization of the onset of distortion-product otoacoustic emissions, and measurement of their latency. J. Acoust. Soc. Am. 100, 1663–1679.
Withnell, R.H., Yates, G.K., 1998. Onset of basilar membrane nonlinearity reflected in cubic distortion tone input–output functions. Hear. Res. 123, 87–96.
Withnell, R.H., Kirk, D.L., Yates, G.K., 1998. Otoacoustic emissions measured with a physically open recording system. J. Acoust. Soc. Am. 104, 350–355.
Withnell, R.H., Yates, G.K., Kirk, D.L., 2000. Changes to low-frequency components of the TEOAE following acoustic trauma to the base of the cochlea. Hear. Res. 139, 1–12.
Withnell, R.H., Shaffer, L.A., Lilly, D.J., 2002. What drives mechanical amplification in the mammalian cochlea? Ear Hear. 23, 49–57.
Withnell, R.H., Shaffer, L.A., Talmadge, C.L., 2003. Generation of DPOAEs in the guinea pig. Hear. Res. 178, 106–117.
Yates, G.K., Withnell, R.H., 1999. The role of intermodulation distortion in transient-evoked otoacoustic emissions. Hear. Res. 136, 49–64.
Zweig, G., Shera, C.A., 1995. The origin of periodicity in the spectrum of evoked otoacoustic emissions. J. Acoust. Soc. Am. 98, 2018–2047.
Zwicker, E., 1986. A hardware cochlear nonlinear preprocessing model with active feedback. J. Acoust. Soc. Am. 80, 146–153.